


PRL-3 induces a positive signaling circuit between glycolysis and activation of STAT1/2

Esten Nymoen Vandsemb¹, Morten Beck Rye^{1,2,3,4}, Ida Johnsen Steiro¹, Samah Elsaadi^{1,3}, Torstein Bade Rø^{1,5}, Tobias Schmidt Slørdahl^{1,6}, Anne-Marit Sponaas¹, Magne Børset^{1,7} and Pegah Abdollahi^{1,3,6} 

¹ Department of Clinical and Molecular Medicine, Faculty of Medicine and Health Sciences, Norwegian University of Science and Technology (NTNU), Trondheim, Norway

² Clinic of Surgery, St. Olavs University Hospital, Trondheim, Norway

³ Clinic of Laboratory Medicine, St. Olavs University Hospital, Trondheim, Norway

⁴ Biocore – Bioinformatics Core Facility, Norwegian University of Science and Technology (NTNU), Trondheim, Norway

⁵ Children's Clinic, St. Olavs University Hospital, Trondheim, Norway

⁶ Clinic of Medicine, St. Olavs University Hospital, Trondheim, Norway

⁷ Department of Immunology and Transfusion Medicine, St. Olavs University Hospital, Norway

Keywords

interferon; metabolism; multiple myeloma; PTP4A3; STAT1/STAT2

Correspondence

P. Abdollahi, Department of Clinical and Molecular Medicine NTNU, 7491

Trondheim, Norway

Tel: +4748437424

E-mail: pegah.abdollahi@ntnu.no

(Received 14 February 2021, revised 28 April 2021, accepted 4 June 2021)

doi:10.1111/febs.16058

Multiple myeloma (MM) is an incurable hematologic malignancy resulting from the clonal expansion of plasma cells. MM cells are interacting with components of the bone marrow microenvironment such as cytokines to survive and proliferate. Phosphatase of regenerating liver (PRL)-3, a cytokine-induced oncogenic phosphatase, is highly expressed in myeloma patients and is a mediator of metabolic reprogramming of cancer cells. To find novel pathways and genes regulated by PRL-3, we characterized the global transcriptional response to PRL-3 overexpression in two MM cell lines. We used pathway enrichment analysis to identify pathways regulated by PRL-3. We further confirmed the hits from the enrichment analysis with *in vitro* experiments and investigated their function. We found that PRL-3 induced expression of genes belonging to the type 1 interferon (IFN-I) signaling pathway due to activation of signal transducer and activator of transcription (STAT) 1 and STAT2. This activation was independent of autocrine IFN-I secretion. The increase in STAT1 and STAT2 did not result in any of the common consequences of increased IFN-I or STAT1 signaling in cancer. Knockdown of STAT1/2 did not affect the viability of the cells, but decreased PRL-3-induced glycolysis. Interestingly, glucose metabolism contributed to the activation of STAT1 and STAT2 and expression of IFN-I-stimulated genes in PRL-3-overexpressing cells. In summary, we describe a novel signaling circuit where the key IFN-I-activated transcription factors STAT1 and STAT2 are important drivers of the increase in glycolysis induced by PRL-3. Subsequently, increased glycolysis regulates the IFN-I-stimulated genes by augmenting the activation of STAT1/2.

Abbreviations

BM, bone marrow; IFN-I, type 1 interferon; ISGs, IFN-stimulated genes; MM, multiple myeloma; PRL, phosphatase of regenerating liver; STAT, signal transducer and activator of transcription.

Introduction

Multiple myeloma (MM) is an incurable hematologic cancer caused by malignant transformation and clonal expansion of plasma cells in the bone marrow (BM). The cancer cells in patients with MM have a diverse set of genetic and other molecular aberrations, but patients suffer from fairly specific clinical traits including anemia, renal failure, and erosion of bone [1–3]. Further, the dynamic interaction between the MM cells and components of the BM microenvironment is crucial for survival and growth of the cancer cells [4].

Phosphatases of regenerating liver (PRLs) constitute a family of three members, PRL-1, PRL-2, and PRL-3, which are often overexpressed in cancer [5]. In contrast to PRL-1 and PRL-2, which are ubiquitously expressed in various normal tissues, expression of PRL-3 is only found in a few cell types (mainly muscle cells) and in cancer cells, which makes it an attractive molecule for targeted cancer treatment [5,6]. Studies have reported various oncogenic roles for PRL-3 in a wide range of solid tumors [7–9] and in hematological malignancies [10–17].

The PRL-3 gene (*PTP4A3*) is expressed at a higher level in malignant plasma cells from MM patients than in plasma cells from healthy donors, and high expression is associated with a poor prognosis [2,14]. Further, a gene expression profiling study of 320 newly diagnosed MM patients identified a subgroup where the main characteristic was high PRL-3 expression [15]. We have previously shown that PRL-3, which is an effector protein downstream of IL-6, protects myeloma cells against apoptosis by activation of the oncoprotein Src and signal transducer and activator of transcription (STAT)3, and by stabilizing the antiapoptotic protein MCL-1 [14,18,19]. We have further introduced PRL-3 as an important regulator of glycolysis in cancer cells of hematological origin [20]. Despite a substantial number of studies implicating PRL-3 as an oncogenic protein, further research is required to define its role in cancer progression [5,6].

To elucidate the role and identify novel pathways regulated by PRL-3 in MM, we characterized the global transcriptomic response to PRL-3 overexpression in the IL-6-dependent cell line (INA-6) and in the IL-6-independent cell line (JJN-3). In both cell lines, we found that PRL-3 induced expression of genes belonging to the type 1 interferon (IFN-I) signaling pathway, and activation of STAT1 and STAT2. This activation was both a response to and a mediator of the increased glycolysis induced by PRL-3.

Results

PRL-3 overexpression leads to increased expression of interferon-regulated genes

To investigate the transcriptional programs regulated by PRL-3 in MM, we performed gene expression analysis of two cell lines overexpressing PRL-3 compared with their respective mock control cells. We used the IL-6-dependent INA-6 and the IL-6-independent JJN-3 cell lines described previously [20]. Myeloma cells are dependent on the microenvironment to survive and proliferate, and the IL-6-dependent cell lines are more similar to patient samples than the myeloma cell lines that are not dependent on IL-6 [21]. We have previously shown that PRL-3 expression can be induced by cytokines in several myeloma cell lines, both IL-6-dependent and IL-6-independent [14]. Hence, we were interested in the transcriptional programs regulated by PRL-3 in both INA-6 and JJN-3. A total number of 487 genes were upregulated in PRL-3 INA-6, while 394 genes were downregulated. In JJN-3, 978 genes were upregulated, whereas 641 genes were downregulated (Fig. 1A,B). The discrepancy in number of differentially expressed genes is likely due to RNA-seq having a better ability to detect low abundance and noncoding transcripts as compared to the predefined set of transcripts detected by microarray technology. In addition, the differences in the biology of the cell lines could also explain some of the variation. To identify pathways regulated by PRL-3 in both cell lines, we used Reactome pathway analysis to pinpoint the common

Fig. 1. Transcriptomic profiling of PRL-3-overexpressing INA-6 and JJN-3 cells indicates activation of the IFN-I signaling pathway. (A) Differentially expressed genes (\log_2 fold change of ≥ 0.5 or ≤ -0.5 and adjusted P -value ≤ 0.05 between PRL-3 and mock cells) presented as volcano plots. (B) Venn diagrams of significantly upregulated and downregulated genes in INA-6 and JJN-3. (C) The top 10 Reactome pathways based on the genes upregulated in the individual cell lines and the 59 genes upregulated in both JJN-3 and INA-6 overexpressing PRL-3. (D) The top 10 predicted transcription factors based on the 59 genes upregulated by PRL-3 in both JJN-3 and INA-6 (top panels) and based on the top 500 genes that correlated with *PTP4A3* in the CoMMpass database (bottom panels), inferred from two different databases (TRRUST and ENCODE TF ChIP-seq) using Enrichr. Blue bars represent STAT2, red represent STAT1, and pathways involving both are shown with a blue and red bar. Both (C) and (D) show the top 10 predicted entities (human signaling pathways or transcription factors) as sorted by unadjusted P -value.

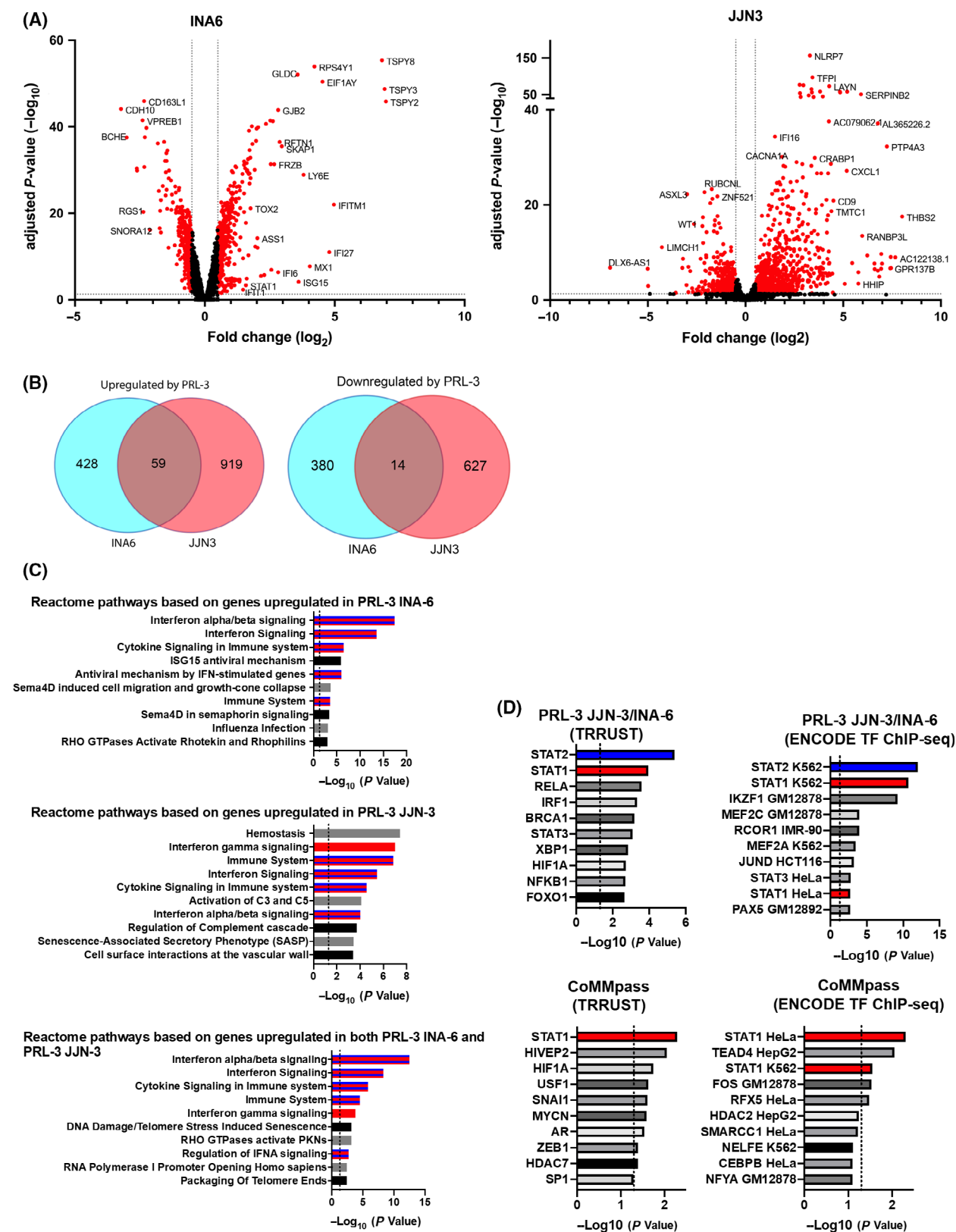


Table 1. 59 genes overexpressed in both PRL-3 INA-6 and PRL-3 JJN-3. Genes known to be induced by type I interferons are shown in bold

ADAM19	IRF9
ADPRH	ISG20
AIM2	LAT2
APH1B	LEPR
ASS1	LGALS1
BLVRA	LILRA2
CCL2	MAGEA10
CD69	MERTK
CHMP5	MIAT
CTAG2	OAS2
EGR1	OASL
EIF2B2	PARP9
F2R	PKD3
FHL1	PFKFB4
GRAP	PNMA5
H1FO	PTP4A3
HEG1	RAB11FIP1
HIST1H2BD	RHOB
HIST1H2BG	RRAGD
HIST2H2AA3	SAT1
HSPA1A	ST3GAL5
HSPB1	STAT1
IFIT3	SWAP70
IL32	SYT11
IRAK2	TAP1
TPST2	TDRD7
USP18	TNFSF10
VIM	TOB1
WSCD1	TPST1
XAF1	

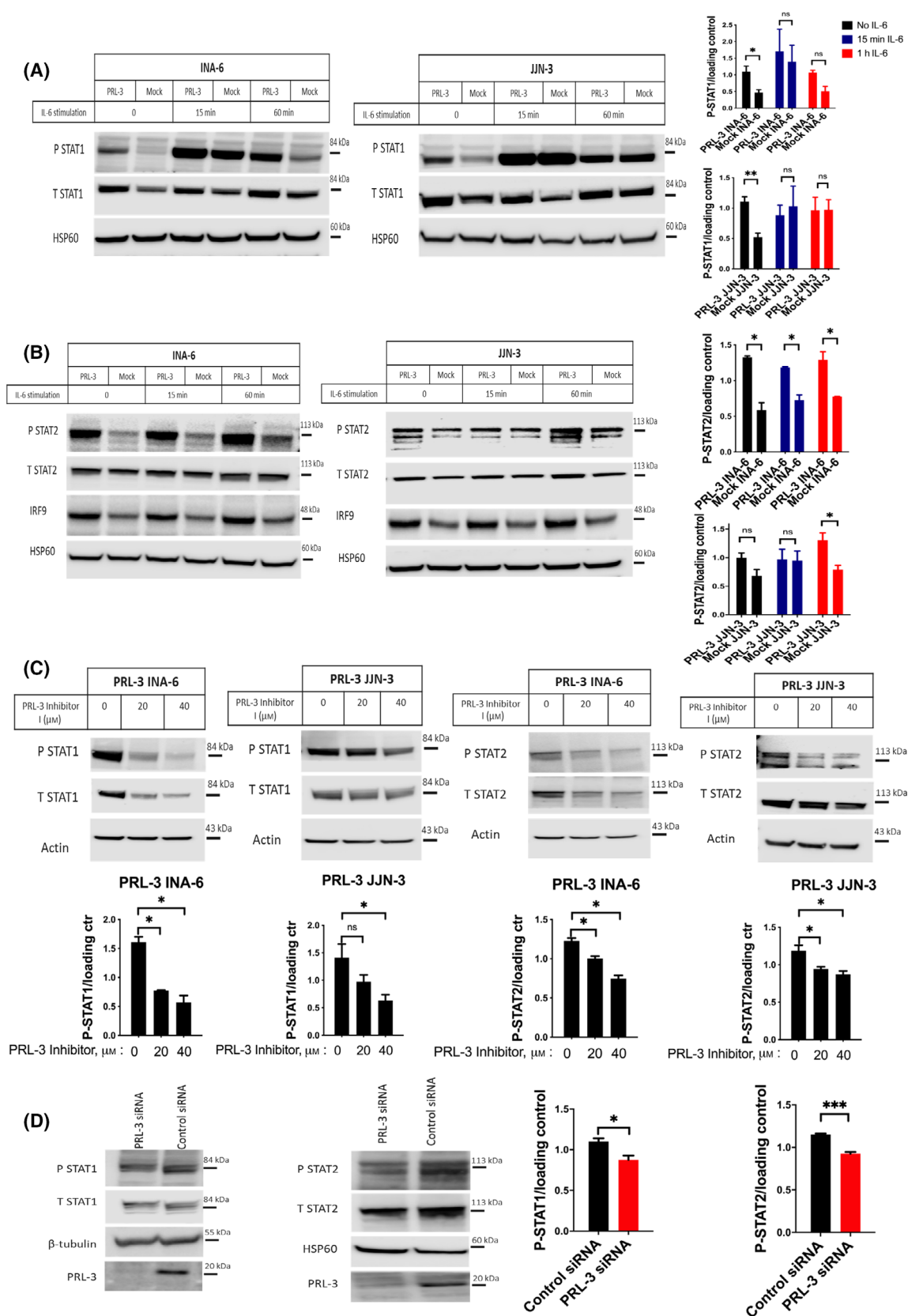
pathways upregulated in both PRL-3 JJN-3 and PRL-3 INA-6 based on the genes upregulated in each cell line, in addition to the genes upregulated in both cell lines (Fig. 1C). Based on the 59 common genes (Table 1) upregulated in both PRL-3 JJN-3 and PRL-3 INA-6, we found that IFN-I-regulated pathways were most enriched. The involvement of IFN-I was also indicated by STAT2 and STAT1 being the top predicted transcription factors of the 59 common genes, based on data from two different databases (Fig. 1D, top). In gene expression data from MM patient samples in the publicly available CoMMpass database, STAT1 was the top predicted

transcription factor based on an analysis of the 500 genes with the highest correlation coefficient with PTP4A3 (Fig. 1D, bottom).

PRL-3 overexpression leads to activation of STAT1 and STAT2 independently of type I interferons

The transcription factors STAT2 and STAT1 are classically activated by IFN-I and regulate the expression of IFN-stimulated genes (ISGs) [22]. This effect is typically mediated by transcription factor complexes made up of STAT1/STAT2 as a heterodimer, or together with IFN regulatory factor 9 (IRF9) forming a heterotrimeric complex called ISGF3 [23]. Based on the enrichment of ISGs in our transcriptomic data, we investigated the activation of these transcription factors in our cells. In both INA-6 and JJN-3 cells, the overexpression of PRL-3 led to increased level of phosphorylated STAT1 and STAT2, although the level of phosphorylated STAT2 was generally lower in JJN-3 than in INA-6 (Fig. 2A,B). Since IL-6 both activates and increases the expression of STAT1, and since PRL-3 is a mediator of IL-6 signaling, we performed experiments in conditions both with and without IL-6. The phosphorylation of STAT1 was as expected responsive to IL-6 stimulation (Fig. 2A), whereas the phosphorylation of STAT2 was less influenced by IL-6. In addition to increased phosphorylation, the total levels of STAT1 were also increased in cells overexpressing PRL-3. Further, PRL-3 increased the total level of IRF9, although it was less influenced by stimulation with IL-6. To investigate whether inhibition of PRL-3 could reverse the activation of STAT1 and STAT2, we treated PRL-3-overexpressing INA-6 and JJN-3 cells with PRL-3 inhibitor 1, which is known to decrease the protein level of PRL-3 [11,20]. As expected, reduced PRL-3 level decreased both active and total levels of STAT1 and STAT2 (Fig. 2C). In accordance with the results using the inhibitor, knockdown of PRL-3

Fig. 2. PRL-3 overexpression leads to activation of STAT1 and STAT2 and increased expression of total IRF9. Western blots showing (A) P-STAT1 and total STAT1 expression, (B) P-STAT2, total STAT2, and total IRF9 expression and the influence of IL-6 in INA-6 and JJN-3 cells as indicated. INA-6 cells were cultured without IL-6 for 90 min prior to reintroduction of 5 ng·mL⁻¹ IL-6. (C) PRL-3-overexpressing INA-6 and JJN-3 cells were treated with 20 and 40 μ M PRL-3 inhibitor 1 for 6 h followed by evaluation of P-STAT1, P-STAT2, and their total expression by western blot. (D) Endogenous PRL-3 was transiently knocked down in INA-6, and protein expression was measured by western blot. The bar graphs in the right panel show the band densitometry normalized to the loading control in the independent biological replicates. Figure (A, B, D) is one representative out of at least three independent experiments. Figure (C) is one representative out of two independent experiments. Error bars show \pm SEM. * P < 0.05, ** P < 0.01, and *** P < 0.001 (two-sample t -test).



using siRNA significantly reduced phosphorylated STAT1 and STAT2 in wild-type INA-6 cells (Fig. 2D). Next, we wanted to explore whether PRL-3-mediated activation of STAT1 and STAT2 was due to the induction of an autocrine loop of IFN-I instigated by PRL-3. None of the IFNs were among the mutually upregulated genes (Table 1) in our transcriptomics data. In addition, we used the Nanostring Human Immunology Kit to quantify the expression of several immune-related genes, including *IFNA1/13*, *IFNA2*, *IFNB1*, and *IFNG* mRNA. Neither PRL-3 INA-6 nor mock INA-6 expressed these IFNs although we confirmed PRL-3-driven upregulation of the ISGs *MX1*, *IFITM1*, and *STAT1* (Fig. 3A). Additionally, we were not able to detect IFN- α 2 and IFN- β at the protein level in neither INA-6 nor JJN-3 cells with ELISA (Fig. 3B). Taken together, our results indicate that PRL-3 mediates activation of STAT1 and STAT2 independent of autocrine IFN production.

STAT1 and STAT2 did not regulate survival in myeloma cells, and overexpression of PRL-3 did not lead to increased susceptibility to either type I interferons and TRAIL or resistance toward doxorubicin

To investigate whether STAT1 and STAT2 could mediate a prosurvival signal in our cell lines, we knocked down the two transcription factors using siRNA. Knocking down the transcription factors individually or in combination did not change the viability of the PRL-3 INA-6 cells assessed by annexin V staining (Fig. 4A). Neither *STAT1* nor *STAT2* expression had a

prognostic impact for MM patients based on data from the CoMMpass study (data not shown). As IFNs can act as both antiapoptotic and proapoptotic factors, we investigated whether increased expression of PRL-3 would change the sensitivity of the cells to IFN-I. No such change in sensitivity was observed, as a high dose of both IFN- α 2 and IFN- β only had minor effects on the cell lines after 48 h of incubation (Fig. 4B). Studies on solid tumors have found that IFN-induced genes and STAT1 are associated with resistance against DNA-damaging agents such as doxorubicin and radiotherapy [24,25]. This was not the case in our cells, as doxorubicin sensitivity was similar in JJN-3 and INA-6 cells overexpressing PRL-3 and in their respective control cells (Fig. 4C). Also, we could not find any difference in susceptibility to TRAIL-induced apoptosis (Fig. 4D), which is regarded as an important mediator of the apoptotic effect of IFN-I in cancer, including MM [26,27].

STAT1/2 activation by PRL-3 increases glycolysis in myeloma cells

We previously published that PRL-3 acts as a critical regulator of glycolysis in MM cells [20]. Even though the role of STAT1/2 is more thoroughly studied in the context of antiviral responses, a few studies have shown that STAT1 indeed can regulate genes involved in glycolysis and metabolism, also in cancer cells [28,29]. Therefore, we hypothesized that PRL-3 might regulate glycolysis through STAT1/STAT2. We first tested whether the IFN-I signaling pathway can induce glycolysis in MM cells. As shown in Fig. 5A, stimulating the IL-6-independent cell line JJN-3 with IFN- β

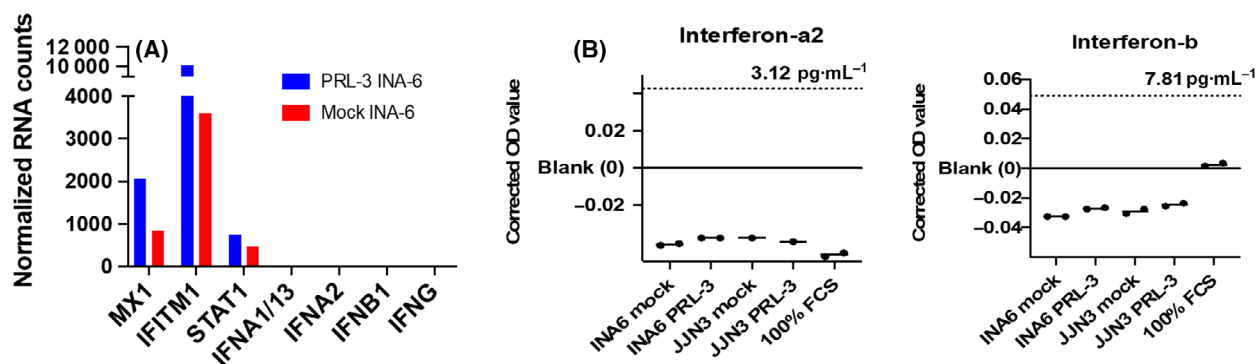


Fig. 3. PRL-3 overexpression does not lead to autocrine secretion of type I interferons. (A) mRNA expression of interferons and ISGs assessed with Nanostring Human Immunology V2. (B) Interferon- α 2 and interferon- β were measured by ELISA in supernatants from JJN-3 and INA-6 cells overexpressing PRL-3 and their respective mock control. The Nanostring analysis in (A) was performed once. Figure (B) is one representative result from two independent experiments with two biological duplicates in each.

enhanced glycolysis, confirming that the IFN signaling pathway can influence metabolism in our cells. Next, we tested our PRL-3-overexpressing INA-6 cells with STAT1 and STAT2 knocked down separately or in combination. All knockdown experiments showed decreased glycolysis, although STAT1 seemed to be more important for the increase in glycolysis than STAT2 (Fig. 5B). Taken together, these results indicate that PRL-3 influences glycolysis through STAT1 and STAT2 activation.

Glucose import and glycolysis contributes to the activation of STAT1 and STAT2 and expression of ISGs

We previously published that PRL-3 acts as an inducer of glycolysis, partly through increasing glucose uptake. We therefore investigated whether the PRL-3-induced STAT1/STAT2 activation occurs through regulation of metabolism. For this purpose, we incubated the PRL-3 and mock cells with various concentrations of glucose. Interestingly, we found that STAT1 and STAT2 were activated in a dose-dependent manner by glucose in PRL-3 INA-6 and PRL-3 JJN-3, while the corresponding mock cells only showed a slight increase in activation of STAT1 and STAT2 (Fig. 6A,B). Activation of STATs can lead to increased transcription of STATs, thus forming a positive feedback circuit [30,31]. This is reflected in the concomitant decrease in both phosphorylated STAT and total STAT in glucose-deprived conditions in our experiments. It is noteworthy that glucose starvation had no effect on total Src level (data not shown). Treating the PRL-3-overexpressing cells with the glycolysis inhibitor 2DG (2 mM) resulted in a visible decrease in phosphorylated STAT1 in both INA-6 and JJN-3, although this was not statistically significant upon quantification (Fig. 6C). We used qPCR to measure some of the differentially expressed ISGs (*IFI27*, *IFIT3*, *IFITM1*, *ISG15*, *ISG20*, and *MX1*) in cells incubated in RPMI media with and without glucose (Fig. 6D). We found that several of the STAT1/STAT2-regulated genes were increased upon addition of glucose. Taken together, our results indicate that higher glycolysis in PRL-3-overexpressing cells induces activation of STAT1 and STAT2 and subsequently increased expression of ISGs.

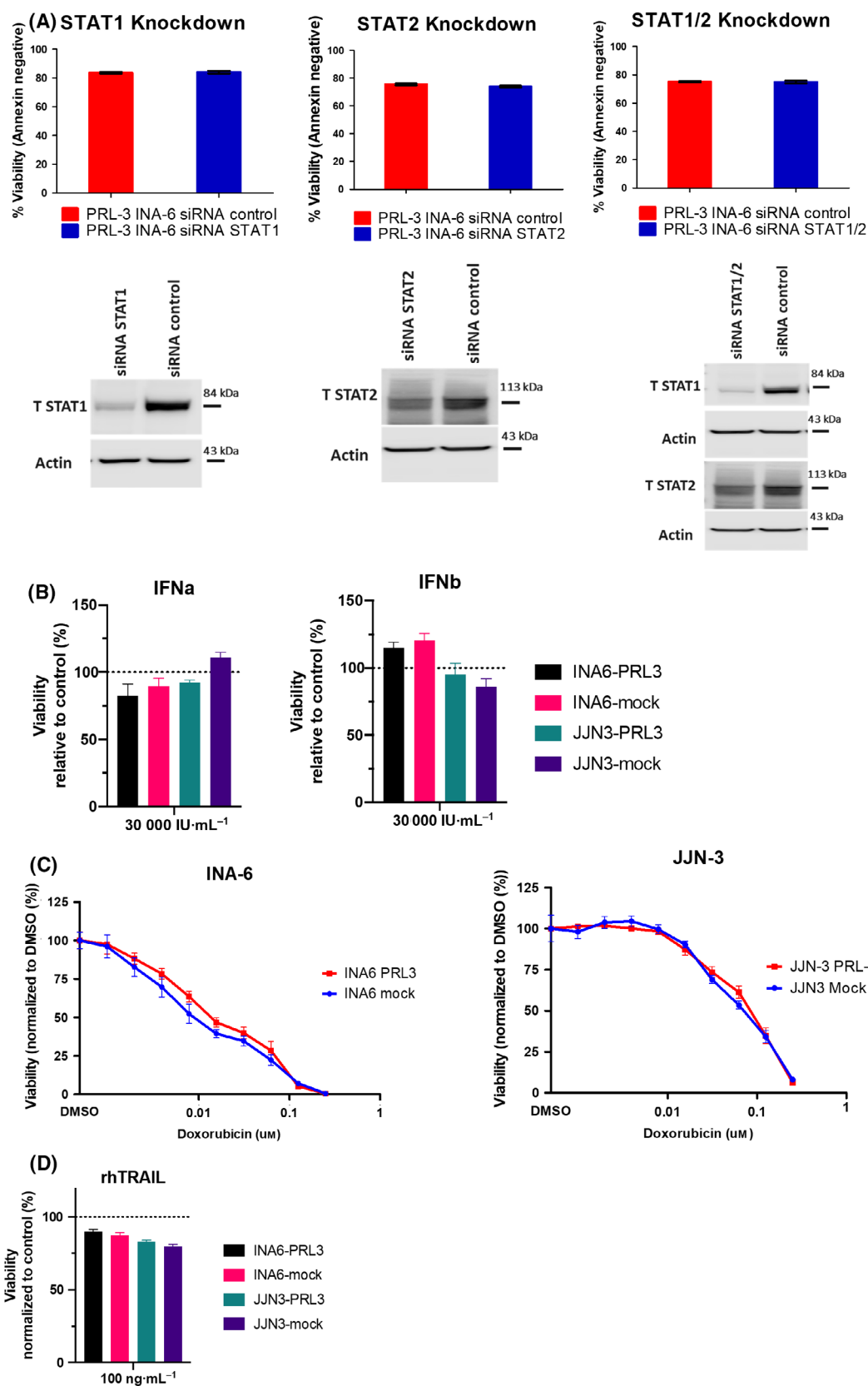
Discussion

In this study, we used transcriptional profiling and found that PRL-3 overexpression led to significant changes in the expression of several hundred genes in

both JJN-3 and INA-6 myeloma cells. The IFN-I signaling pathway was the most prominent signaling pathway induced by PRL-3 overexpression when assessing gene expression of the two cell lines together. Interestingly, the activation of this pathway was positively modulated by the increase in glycolysis and glucose import that is induced by PRL-3 overexpression, revealing a complex interplay between cell signaling, cellular metabolism, and cancer biology.

IFNs constitute a protein family of several cytokines that can be grouped into three types that bind to different receptors. The IFN-I family induces the phosphorylation of STAT1 and STAT2 and can subsequently trigger the formation of the ISGF3 transcription factor complex, composed of phosphorylated STAT1 and STAT2 together with IRF9. Activation of these transcription factors leads to expression of ISGs. In our study, we found that PRL-3 overexpression increases the phosphorylation of STAT1 and STAT2, as well as the total expression of IRF9. Interestingly, the activation of the IFN-I signaling pathway by PRL-3 was independent of autocrine IFN-I secretion, which to our knowledge is a novel observation in MM. We observed concomitant activation of both STAT1 and STAT2, and as the latter is usually not activated by IL-6, it suggests that PRL-3 mediates crosstalk between the IL-6 and IFN-I signaling pathways. This expands on the previous findings from us and others showing that PRL-3 augments signal downstream of IL-6 in MM cells [18,19,32].

IFN-I signaling, and consequently STAT1 and STAT2, are mostly studied in the context of antiviral and antitumor responses. The literature on STAT2 in cancer is limited, whereas more studies have been performed on STAT1. However, the role of STAT1 in tumorigenesis is complex and it has been linked to both good prognosis [33,34] and disease progression [35,36]. Among the most consistent reports on STAT1 as an oncogene is its role in resistance toward several cancer treatment modalities, including radiotherapy and chemotherapy [25,37,38,39,40,41]. In our study, the activation of STAT1 and STAT2 induced by PRL-3 overexpression did not lead to doxorubicin resistance as observed in other studies in solid tumors [38] nor did it change the susceptibility toward TRAIL-induced apoptosis, commonly associated with IFN-induced signaling [26,42,43]. Knocking down STAT1 and STAT2 individually or in combination did not alter the viability of myeloma cells, and overexpression of PRL-3 did not lead to a substantial change in viability in response to exogenous IFN-I stimulation. Therefore, we were not able to conclude that the increased activity in the IFN-I signaling pathway observed in our cells led to



any of the most common consequences of increased IFN-I signaling or STAT1 activation reported in the literature.

The effect of IFNs and their downstream signaling molecules in MM is far from fully understood. IFN- α was previously used to treat MM, but with significant side effects and a varying degree of efficacy, it is no longer a commonly used drug for this cancer [44]. Nevertheless, several ISGs are overexpressed in MM cells [45–47], and a recent article comparing gene expression signatures of primary myeloma cells with myeloma cell lines found that interferon response genes were enriched in the patient samples [21]. Hence, a better understanding of IFN-I signaling in myeloma is still of clinical and biological interest. Even though activation of STAT1 by PRL family members has been reported by us [18] and others [32,48], the biological consequence and mechanism of activation have not been investigated. We have previously shown that PRL-3 is important for viability of myeloma cells [18] and can regulate cancer cell metabolism by increasing glucose import and glycolysis [20]. In this study, we found that knockdown of either STAT1 or STAT2 reduced PRL-3-mediated glycolysis but not viability. This fits with a study in a human squamous carcinoma cell line, which found a strong association between STAT1 and genes regulating glycolysis [28]. In addition, we discovered that blocking glycolysis by either glucose starvation or with 2DG disrupted the STAT1/STAT2 phosphorylation and induction of ISGs in PRL-3-overexpressing cells. Our results show that PRL-3 can increase STAT1- and STAT2-mediated signaling independently of autocrine IFN-I. We also show that this pathway is both modulated by the increased metabolic activity and contributes to the increased glucose consumption induced by PRL-3 overexpression. Metabolism is regulated, at least in part, independently of cell division [49]. Thus, cells require signals that drive altered metabolism, as well as increased cell division, for cells to proliferate successfully over time. In the absence of metabolic adaptation to proliferation, cells might end up being atrophied and less functional [50]. In this study, we

present evidence that the activation of STAT1/STAT2 by PRL-3 promotes cell fitness mainly by increasing glycolysis. STAT1/STAT2 did not have any direct effect on cell viability or induction of apoptosis. Whether our results apply to primary cells or other cell types is not known. Nonetheless, our results indicate that investigation of PRL-3 in a viral infection model would be interesting.

In summary, we describe a novel signaling loop where the key IFN-activated transcription factors STAT1 and STAT2 are important drivers of the increase in glycolysis induced by PRL-3. Subsequently, increased glycolysis regulates the IFN-I-stimulated genes by augmented activation of STAT1 and STAT2.

Materials and methods

Cell culture

The human myeloma cell lines INA-6 and JJN-3 were a gift from M. Gramatzki, University of Erlangen-Nurnberg, Germany, and I.M. Franklin, University of Birmingham, UK, respectively. New cultures of cells were seeded at least every 4 months from vials aliquoted with cells propagated shortly after receiving the cells from their described original source, and they were regularly tested to ensure the absence of mycoplasma. All cells were grown in RPMI 1640 supplemented with 0.68 mM L-glutamine and 10% heat-inactivated fetal calf serum (FCS). INA-6 was cultured in media with 1 ng·mL^{−1} IL-6. Cells were cultured at 37 °C in a humidified atmosphere with 5% CO₂, and growth media were replenished twice weekly. In order to deplete cells of IL-6 before experiments, they were washed three times with Hanks' balanced salt solution (HBSS; Sigma-Aldrich, St. Louis, MO, USA). When glucose starvation was performed, cells were grown in glucose-free RPMI 1640 medium (Thermo Fisher Scientific, MA, USA).

Antibodies, cytokines, and other reagents

IL-6 was from Biosource (Camarillo, CA, USA). PRL-3 inhibitor I (5-[[5-Bromo-2-[(2-bromophenyl)methoxy]phenyl]methylene]-2-thioxo-4-thiazolidinone) and IFN- α 2 human (#SRP4594) were from Sigma-Aldrich. PBMN-ires-

Fig. 4. STAT1 and STAT2 are not involved in resistance toward apoptotic stimuli and are not important for cell viability in PRL-3-overexpressing cells. (A) STAT1, STAT2, or both STAT1 and STAT2 in combination were transiently knocked down using siRNA and viable cells shown as percentage negative for annexin V staining. Bottom panel shows western blots confirming knockdown efficiency. CellTiter-Glo was used to assess viability in PRL-3-overexpressing and mock control cells cultured with (B) 30 000 IU·mL^{−1} IFN- β or IFN- α 2 for 48 h, (C) increasing concentration of doxorubicin for 72 h and (D) recombinant human TRAIL (100 ng·mL^{−1}) overnight. Figure (A) is one representative out of two independent experiments. Both figure (B and D) show one representative out of three independent experiments. Error bars show \pm SD. Figure (C) is a combination of three independent experiments, each with three technical replicates and error bars show \pm SEM.

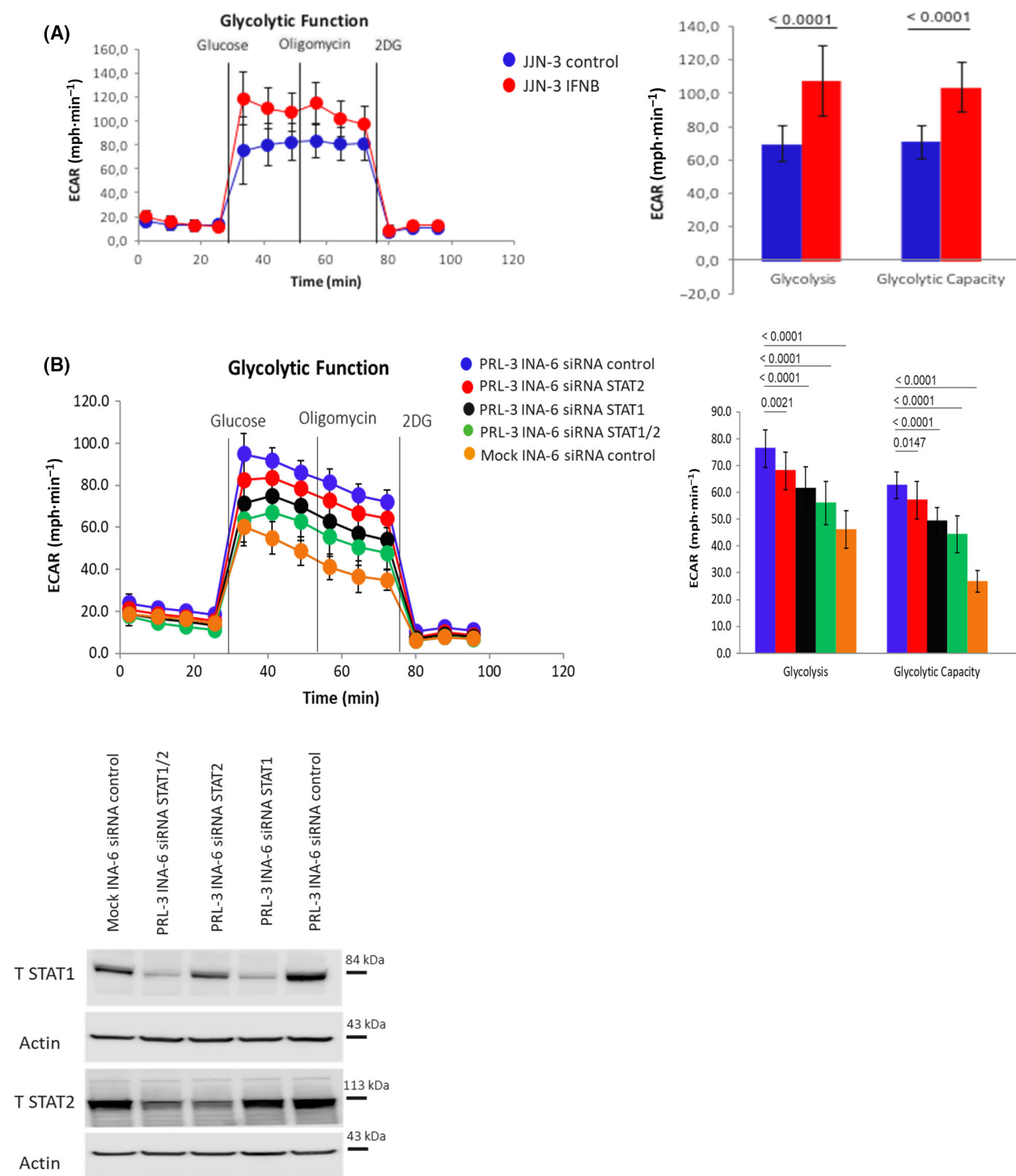
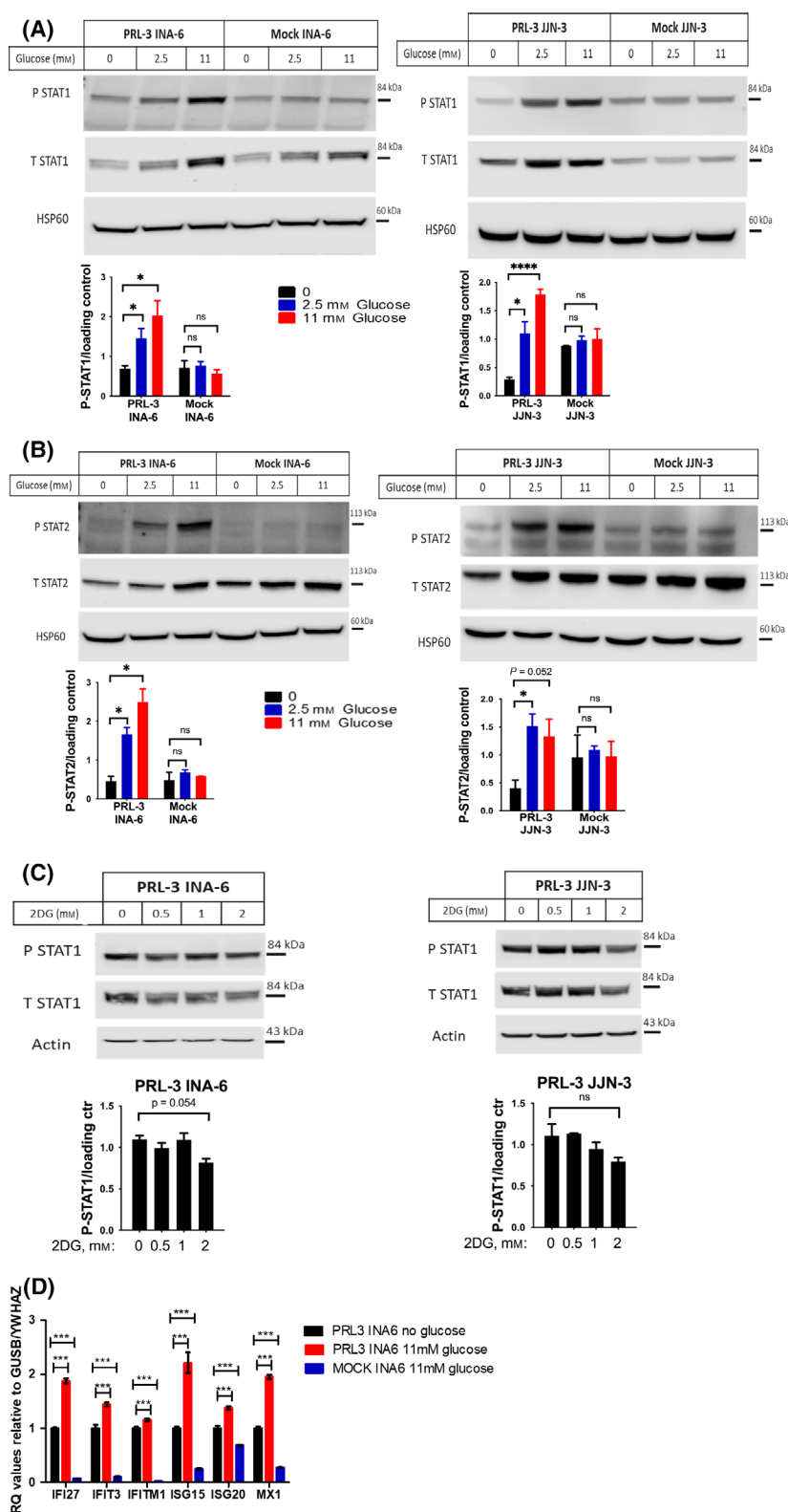


Fig. 5. STAT1 and STAT2 regulate glycolysis in MM. Glycolysis parameters including glycolysis and glycolysis capacity were measured by Seahorse XF Bioanalyzer in (A) cytokine-independent human myeloma JLN-3 cells after overnight stimulation with 500 IU·mL⁻¹ IFN- β . (B) INA-6 PRL-3 cells after transient knockdown of STAT1, STAT2, or STAT1 and STAT2 in combination using siRNA. Bottom panel shows western blot confirming knockdown efficiency. Error bars show \pm SD. Statistical significance was determined by the two-sample *t*-test.



GFP was a gift from Garry Nolan (Addgene 130 plasmid # 1736, Watertown, MA, USA). pLenti CMV Puro DEST (w118-1) was a gift from Eric Campeau & Paul Kaufman (Addgene plasmid # 17452[51]). Antibodies against P Y701 STAT1 (#9167), β -actin (#4967), P Tyr690 STAT2 (#88410), Total STAT1 (#14994) and HSP60 (#12165) were from Cell Signaling Technology (BioNordika AS, Oslo, Norway). Antibodies against PRL-3 (318; #sc-130355), ISGF-3 γ p48 (IRF9; sc-365893), β -tubulin (sc-5274 HRP), and total STAT2 (sc-514193) were from Santa Cruz Biotechnology (Dallas, TX, USA). All antibodies were used at 1 : 1000 dilution. Doxorubicin (#S1208), recombinant human TRAIL (#752906), and recombinant human IFN- β (#300-02BC) were from Selleckchem, Biolegend (London, UK), and PeproTech (Stockholm, Sweden), respectively.

Transduction for PRL-3 overexpression

PRL-3 was overexpressed in INA-6 by retroviral transduction as previously described [19]. pBMN-PTP4A3-ires-GFP and BMN-ires-GFP (control plasmid) were used to establish cells expressing WT PRL-3 (PRL-3 INA-6) and control vector (mock INA-6), respectively. PRL-3 in JJN-3 cells was expressed by lentiviral transduction. pLenti CMV Puro DEST-PTP4A3 and pLenti CMV Puro DEST (control plasmid) were used to establish PRL-3 JJN-3 and mock JJN-3, respectively.

Microarray gene expression analysis

RNA was isolated from four independent cultures of PRL-3 INA-6 and mock INA-6 using RNeasy Mini Kit (Qiagen, Crawley, UK) as previously described [18]. The microarray gene expression analysis followed standard protocols. In brief, cRNA was prepared with Ambion's Illumina® TotalPrep™ RNA Amplification Kit (Thermo Fisher), using 300 ng total RNA as input material. For each sample, the biotin-labeled cRNA concentrations were checked with NanoDrop (Thermo Fisher) before 750 ng was hybridized to HumanHT-12 Expression BeadChips (Illumina Inc., San Diego, CA, USA). Only probes abiding to the Illumina detection *P*-value of 0.01 in at least one sample were included in further analyses, using the LIMMA (v. 3.16.8) Bioconductor package [52]. The *P*-value was adjusted for multiple hypothesis testing using FDR (Benjamini and Hochberg). Probe intensity values were log₂-transformed and quantile-normalized before differential expression analysis.

RNA-sequencing gene expression analysis

RNA was isolated from four independent cultures of PRL-3 JJN-3 and mock JJN-3 using RNeasy Mini Kit (Qiagen, Crawley, UK) as previously described (5). RNA-sequencing libraries were generated using SENSE mRNA-Seq Library Prep Kit according to the manufacturer's instructions

(Lexogen GmbH, Vienna, Austria). In brief, 500 ng of total RNA was prepared and incubated with magnetic beads coated with oligo-dT, followed by removal of all other RNAs except mRNA was removed by washing. Library preparation was then initiated by random hybridization of starter/stopper heterodimers to the poly (A) RNA still bound to the magnetic beads. These starter/stopper heterodimers contain Illumina-compatible linker sequences. A single-tube reverse transcription and ligation reaction extends the starter to the next hybridized heterodimer, where the newly synthesized cDNA insert was ligated to the stopper. Second-strand synthesis was performed to release the library from the beads. The resulting double-stranded library was purified and amplified (12 PCR cycles) prior to adding the adaptors and indexes. Finally, libraries were purified using the Mag-Bind RXNPure Plus beads (Omega Bio-tek, Norcross, GA, USA), quantitated by qPCR using KAPA Library Quantification Kit (Kapa Biosystems, Inc., Boston, MA, USA), and validated using Agilent High Sensitivity DNA Kit on a Bioanalyzer (Agilent Technologies, Santa Clara, CA, USA). The size range of the DNA fragments was measured to be in the range of approximately 200–400 bp and peaked around 250 bp.

Libraries were normalized and pooled to a final concentration of 2.6 pM and subjected to clustering on a NextSeq 500 High-Output Flow Cell (Illumina, Inc.). Finally, single-read sequencing was performed for 75 cycles on a NextSeq 500 instrument (Illumina, Inc.), according to the manufacturer's instructions. Base calling was done on the NS500 instrument by RTA 2.4.6. FASTQ files were generated using BCL2FASTQ2 Conversion Software v2.17 (Illumina, Inc.). The Salmon software was used to align the reads to the human transcriptome [53]. Differentially expressed genes were identified with DESeq2 and SARTools [54,55].

Knockdown by siRNA nucleofection

Prior to gene knockdown by siRNA, cells were grown with low density. In total, 5×10^6 cells were pelleted, and the pellet was resuspended in transfection buffer [Amaxa® Cell Line Nucleofector® Kit R (Lonza, Basel, Switzerland)]. Cells were added to separate nucleofection cuvettes containing 5 μ M of siRNA and transfected by a Nucleofector™ II device (Lonza). Program X-001 was used for INA-6. siRNAs used were SMARTpool ON-TARGETplus from Dharmacon (Lafayette, CO, USA) against: STAT1 (L-003543-00-0005), STAT2 (L-012064-00-0005), PTP4A3 (L-006859-00-0005), and Non-targeting Control Pool (D-001810-10-05). Western blot was used to confirm knockdown after 48 hours.

Immunoblotting

Cells were treated as indicated, and immunoblotting was performed as previously described [18]. Images were acquired using LI-COR Odyssey Fc and analyzed with

IMAGE STUDIO software (LI-COR, Lincoln, Nebraska). Densitometry was done with FIJI [56].

Cell viability and apoptosis assay

Viability was estimated using CellTiter-Glo® Luminescent Cell Viability Assay (Promega, Fitchburg, WI, USA) according to the manufacturer's instructions. The luminescent signal was recorded with a Victor3 plate reader and Wallac 1420 Work Station software (PerkinElmer Inc., Waltham, MA, USA). Apoptosis was evaluated using Annexin V–Alexa Fluor™ 647 binding (A23204; Thermo Fisher), as previously described [18].

Glycolytic flux

Glycolytic function in cells was measured using glycolysis stress test in Seahorse XF96 Bioanalyzer (Seahorse Bioscience, North Billerica, MA, USA) according to the manufacturer's instructions. Briefly, 96-well Seahorse cell culture plates (Seahorse Bioscience, North Billerica, MA, USA) were coated with Cell-Tak (Corning Inc., Corning, NY, USA) in advance. To hydrate a sensor cartridge, 200 µL of distilled sterile water was added to each well of the XF Utility Plate. The XF Sensor Cartridge was placed on top of the utility plate and incubated overnight in 37 °C without CO₂. 45 min before experiment, water was replaced with Seahorse Calibrant solution.

On the day of the experiment, assay medium was prepared by supplementing Seahorse XF Base Medium (102353-100; Seahorse Bioscience) with 2 mM glutamine, warming it up to 37 °C and setting the pH to 7.4 with 0.1 N NaOH. 25×10^3 cells/50 µL assay media were seeded per well and incubated for approximately 30 min at 37 °C without CO₂ to ensure that the cells had completely attached. 130 µL of warm assay medium was gently added along the side of each well to get a final volume of 180 µL.

Glucose (G7021; Sigma-Aldrich), oligomycin (O4876; Sigma-Aldrich), and 2-deoxy-D-glucose (D8375; Sigma-Aldrich) were loaded into port A, port B, and port C of a hydrated sensor cartridge, respectively. Final concentration used for glucose, oligomycin, and 2-deoxy-D-glucose was 10 mM, 1 µM, and 50 µM, respectively.

Following calibration and equilibration, the cell culture microplate was placed in the Seahorse bioanalyzer. The program used for measuring glycolytic flux consisted of a 2-min mixture, followed by a 5-min measurement after each injection. Data were analyzed using the Agilent Seahorse Analyzers Wave 2.6 (Seahorse Bioscience, North Billerica, MA, USA).

Nanostring analysis

The nCounter Human Immunology v2 Kit and nCounter Technology (Nanostring Technologies, Seattle, WA, USA) was used following the manufacturer's protocol to quantify

mRNA expression. The experiment was performed using the nCounter Prep Station and nCounter Digital Analyzer with the standard mRNA gene expression experiment protocol provided by Nanostring Technologies. Briefly, 100 ng total RNA from myeloma cell lines was hybridized with reporter probes overnight. Calculations of transcript numbers were done with the nSolver Analysis Software (Nanostring Technologies). Sample data were normalized against the positive controls and housekeeping genes in the kit.

ELISA

IFN-β and IFN-α2 in supernatants from cell lines were detected with Human IFN-alpha 2/IFNA2 DuoSet ELISA (DY9345-05; R&D Systems, Minneapolis, MN, USA) and Human IFN-beta DuoSet ELISA (DY814-05; R&D Systems (Minneapolis, MN, USA)) following the instructions from the manufacturer. Optical density was determined using iMark™ Microplate Absorbance Reader (Bio-Rad, Hercules, CA, USA).

Data analysis and statistics

The GRAPHPAD PRISM (version 5 or 8; GraphPad Software Inc., San Diego, CA, USA) was used for statistical analyses and generation of most figures. Statistical tests were used as indicated in the figure legends. Gene set enrichment analyses were done with Enrichr [57,58] for both the gene expression data derived from cell lines and gene expression data from the CoMMpass study. RNA-seq data on purified MM cells were downloaded from the CoMMpass interim analysis 13 (IA13) release (<https://research.themmmf.org>). Correlation coefficients were calculated with a custom script. Differentially expressed genes from the gene expression analysis of JJN-3 and INA-6 cell lines were defined as genes with an adjusted *P*-value < 0.05, and a log₂ fold change of more than +0.5 or less than −0.5. In the RNA-seq dataset with JJN-3 cells, transcripts with a base mean of < 10 were excluded. In Table 1, genes in bold are genes upregulated with a fold change of more than 10 by type I interferons in two or more independent datasets in the Interferome database[59].

Acknowledgements

This work was supported by the NTNU and the Liaison Committee for Education, Research, and Innovation in Central Norway, Rakel og Otto Bruuns legat, and Kreftfondet at St Olavs Hospital. We thank Berit Størdal, Glenn Buene, and Hanne Hella for excellent technical support. The gene microarray and RNA-sequencing service was provided by the Genomics Core Facility (GCF), Norwegian University of Science and Technology (NTNU). GCF is funded by the Faculty of Medicine and Health Sciences at NTNU and Central Norway Regional Health Authority. Some of

the included data were generated as part of the MM Research Foundation Personalized Medicine Initiatives (<https://research.themmr.org>).

Conflict of interest

The author declares no conflict of interest.

Data accessibility

Gene expression data are available at ArrayExpress with accession numbers: E-MTAB-10437 and E-MTAB-10436.

Author contribution

ENV and PA were instrumental in study design, in laboratory work, and in writing the manuscript. MBR contributed to bioinformatics analysis, and writing and reviewing the manuscript. SE and IS contributed to study design and laboratory work, and wrote the manuscript. TSS, TBR, and A-MS contributed to study planning and reviewed the manuscript. MB, ENV, and PA conceptualized and coordinated the study and wrote the manuscript.

Peer Review

The peer review history for this article is available at <https://publons.com/publon/10.1111/febs.16058>.

References

- 1 Kumar SK, Rajkumar V, Kyle RA, van Duin M, Sonneveld P, Mateos MV, Gay F & Anderson KC (2017) Multiple myeloma. *Nat Rev Dis Primers* **3**, 17046.
- 2 Abdollahi P, Kohn M & Borset M (2021) Protein tyrosine phosphatases in multiple myeloma. *Cancer Lett* **501**, 105–113.
- 3 Borset M, Sundan A, Waage A & Standal T (2020) Why do myeloma patients have bone disease? A historical perspective. *Blood Rev* **41**, 100646.
- 4 Kawano Y, Moschetta M, Manier S, Glavey S, Gorgun GT, Roccato AM, Anderson KC & Ghobrial IM (2015) Targeting the bone marrow microenvironment in multiple myeloma. *Immunol Rev* **263**, 160–172.
- 5 Campbell AM & Zhang ZY (2014) Phosphatase of regenerating liver: a novel target for cancer therapy. *Expert Opin Ther Tar* **18**, 555–569.
- 6 Bessette DC, Qiu DX & Pallen CJ (2008) PRL PTPs: mediators and markers of cancer progression. *Cancer Metast Rev* **27**, 231–252.
- 7 Tamagawa H, Oshima T, Yoshihara K, Watanabe T, Numata M, Yamamoto N, Tuschida K, Shiozawa M, Morinaga S, Akaike M *et al.* (2012) The expression of the phosphatase regenerating liver 3 gene is associated with outcome in patients with colorectal cancer. *Hepatogastroenterology* **59**, 2122–2126.
- 8 Wang L, Peng L, Dong B, Kong L, Meng L, Yan L, Xie Y & Shou C (2006) Overexpression of phosphatase of regenerating liver-3 in breast cancer: association with a poor clinical outcome. *Ann Oncol* **17**, 1517–1522.
- 9 Vandsemb EN, Bertilsson H, Abdollahi P, Storkersen O, Vatsveen TK, Rye MB, Ro TB, Borset M & Slordahl TS (2016) Phosphatase of regenerating liver 3 (PRL-3) is overexpressed in human prostate cancer tissue and promotes growth and migration. *J Transl Med* **14**, 71.
- 10 Qu S, Liu B, Guo X, Shi H, Zhou M, Li L, Yang S, Tong X & Wang H (2014) Independent oncogenic and therapeutic significance of phosphatase PRL-3 in FLT3-ITD-negative acute myeloid leukemia. *Cancer* **120**, 2130–2141.
- 11 Zhou J, Bi C, Chng WJ, Cheong LL, Liu SC, Mahara S, Tay KG, Zeng Q, Li J, Guo K *et al.* (2011) PRL-3, a metastasis associated tyrosine phosphatase, is involved in FLT3-ITD signaling and implicated in anti-AML therapy. *PLoS One* **6**, e19798.
- 12 Zhou J, Chong PS, Lu X, Cheong LL, Bi C, Liu SC, Zhou Y, Tan TZ, Yang H, Chung TH *et al.* (2014) Phosphatase of regenerating liver-3 is regulated by signal transducer and activator of transcription 3 in acute myeloid leukemia. *Exp Hematol* **42**, 1041–1052.e1–2.
- 13 Zhou J, Cheong LL, Liu SC, Chong PS, Mahara S, Bi C, Ong KO, Zeng Q & Chng WJ (2012) The pro-metastasis tyrosine phosphatase, PRL-3 (PTP4A3), is a novel mediator of oncogenic function of BCR-ABL in human chronic myeloid leukemia. *Mol Cancer* **11**, 72.
- 14 Fagerli UM, Holt RU, Holien T, Vaatsveen TK, Zhan F, Egeberg KW, Barlogie B, Waage A, Aarset H, Dai HY *et al.* (2008) Overexpression and involvement in migration by the metastasis-associated phosphatase PRL-3 in human myeloma cells. *Blood* **111**, 806–815.
- 15 Broyl A, Hose D, Lokhorst H, de Knecht Y, Peeters J, Jauch A, Bertsch U, Buijs A, Stevens-Kroef M, Beverloo HB *et al.* (2010) Gene expression profiling for molecular classification of multiple myeloma in newly diagnosed patients. *Blood* **116**, 2543–2553.
- 16 Hjort MA, Abdollahi P, Vandsemb EN, Fenstad MH, Lund B, Slordahl TS, Borset M & Ro TB (2018) Phosphatase of regenerating liver-3 is expressed in acute lymphoblastic leukemia and mediates leukemic cell adhesion, migration and drug resistance. *Oncotarget* **9**, 3549–3561.
- 17 Hjort MA, Hov H, Abdollahi P, Vandsemb EN, Fagerli UM, Lund B, Slordahl TS, Borset M & Ro TB

- (2018) Phosphatase of regenerating liver-3 (PRL-3) is overexpressed in classical Hodgkin lymphoma and promotes survival and migration. *Exp Hematol Oncol* **7**, 8.
- 18 Slordahl TS, Abdollahi P, Vandsemb EN, Rampa C, Misund K, Baranowska KA, Westhlin M, Waage A, Ro TB & Borset M (2016) The phosphatase of regenerating liver-3 (PRL-3) is important for IL-6-mediated survival of myeloma cells. *Oncotarget* **7**, 27295–27306.
 - 19 Abdollahi P, Vandsemb EN, Hjort MA, Misund K, Holien T, Sponaas AM, Ro TB, Slordahl TS & Borset M (2017) Src family kinases are regulated in multiple myeloma cells by phosphatase of regenerating liver-3. *Mol Cancer Res* **15**, 69–77.
 - 20 Abdollahi P, Vandsemb EN, Elsaadi S, Rost LM, Yang R, Hjort MA, Andreassen T, Misund K, Slordahl TS, Ro TB *et al.* (2021) Phosphatase of regenerating liver-3 regulates cancer cell metabolism in multiple myeloma. *FASEB J* **35**, e21344.
 - 21 Sarin V, Yu K, Ferguson ID, Gugliemini O, Nix MA, Hann B, Sirota M & Wiita AP (2020) Evaluating the efficacy of multiple myeloma cell lines as models for patient tumors via transcriptomic correlation analysis. *Leukemia* **34**, 2754–2765.
 - 22 Stark GR, Kerr IM, Williams BR, Silverman RH & Schreiber RD (1998) How cells respond to interferons. *Annu Rev Biochem* **67**, 227–264.
 - 23 Schneider WM, Chevillotte MD & Rice CM (2014) Interferon-stimulated genes: a complex web of host defenses. *Annu Rev Immunol* **32**, 513–545.
 - 24 Rickardson L, Fryknas M, Dhar S, Lovborg H, Gullbo J, Rydaker M, Nygren P, Gustafsson MG, Larsson R & Isaksson A (2005) Identification of molecular mechanisms for cellular drug resistance by combining drug activity and gene expression profiles. *Br J Cancer* **93**, 483–492.
 - 25 Weichselbaum RR, Ishwaran H, Yoon T, Nuyten DS, Baker SW, Khodarev N, Su AW, Shaikh AY, Roach P, Kreike B *et al.* (2008) An interferon-related gene signature for DNA damage resistance is a predictive marker for chemotherapy and radiation for breast cancer. *Proc Natl Acad Sci USA* **105**, 18490–18495.
 - 26 Crowder C, Dahle O, Davis RE, Gabrielsen OS & Rudikoff S (2005) PML mediates IFN- α -induced apoptosis in myeloma by regulating TRAIL induction. *Blood* **105**, 1280–1287.
 - 27 Chawla-Sarkar M, Lindner DJ, Liu YF, Williams BR, Sen GC, Silverman RH & Borden EC (2003) Apoptosis and interferons: role of interferon-stimulated genes as mediators of apoptosis. *Apoptosis* **8**, 237–249.
 - 28 Pitroda SP, Wakim BT, Sood RF, Beveridge MG, Beckett MA, MacDermid DM, Weichselbaum RR & Khodarev NN (2009) STAT1-dependent expression of energy metabolic pathways links tumour growth and radioresistance to the Warburg effect. *BMC Med* **7**, 68.
 - 29 Sisler JD, Morgan M, Raje V, Grande RC, Derecka M, Meier J, Cantwell M, Szczepanek K, Korzun WJ, Lesnfsky EJ *et al.* (2015) The signal transducer and activator of transcription 1 (STAT1) inhibits mitochondrial biogenesis in liver and fatty acid oxidation in adipocytes. *PLoS One* **10**, e0144444.
 - 30 Cheon H, Holvey-Bates EG, Schoggins JW, Forster S, Hertzog P, Imanaka N, Rice CM, Jackson MW, Junk DJ & Stark GR (2013) IFN β -dependent increases in STAT1, STAT2, and IRF9 mediate resistance to viruses and DNA damage. *EMBO J* **32**, 2751–2763.
 - 31 Michalska A, Blaszczyk K, Wesoly J & Bluyssen HAR (2018) A positive feedback amplifier circuit that regulates interferon (IFN)-stimulated gene expression and controls type I and type II IFN responses. *Front Immunol* **9**, 1135.
 - 32 Chong PSY, Zhou J, Lim JSL, Hee YT, Chooi JY, Chung TH, Tan ZT, Zeng Q, Waller DD, Sebag M *et al.* (2019) IL6 promotes a STAT3-PRL3 feedforward loop via SHP2 repression in multiple myeloma. *Cancer Res* **79**, 4679–4688.
 - 33 Hosui A, Klover P, Tatsumi T, Uemura A, Nagano H, Doki Y, Mori M, Hiramatsu N, Kanto T, Hennighausen L *et al.* (2012) Suppression of signal transducers and activators of transcription 1 in hepatocellular carcinoma is associated with tumor progression. *Int J Cancer* **131**, 2774–2784.
 - 34 Widschwendter A, Tonko-Geymayer S, Welte T, Daxenbichler G, Marth C & Doppler W (2002) Prognostic significance of signal transducer and activator of transcription 1 activation in breast cancer. *Clin Cancer Res* **8**, 3065–3074.
 - 35 Duarte CW, Willey CD, Zhi D, Cui X, Harris JJ, Vaughan LK, Mehta T, McCubrey RO, Khodarev NN, Weichselbaum RR *et al.* (2012) Expression signature of IFN/STAT1 signaling genes predicts poor survival outcome in glioblastoma multiforme in a subtype-specific manner. *PLoS One* **7**, e29653.
 - 36 Khodarev N, Ahmad R, Rajabi H, Pitroda S, Kufe T, McClary C, Joshi MD, MacDermid D, Weichselbaum R & Kufe D (2010) Cooperativity of the MUC1 oncoprotein and STAT1 pathway in poor prognosis human breast cancer. *Oncogene* **29**, 920–929.
 - 37 Fryknas M, Dhar S, Oberg F, Rickardson L, Rydaker M, Goransson H, Gustafsson M, Pettersson U, Nygren P, Larsson R *et al.* (2007) STAT1 signaling is associated with acquired crossresistance to doxorubicin and radiation in myeloma cell lines. *Int J Cancer* **120**, 189–195.
 - 38 Khodarev NN, Roach P, Pitroda SP, Golden DW, Bhayani M, Shao MY, Darga TE, Beveridge MG, Sood RF, Sutton HG *et al.* (2009) STAT1 pathway

- mediates amplification of metastatic potential and resistance to therapy. *PLoS One* **4**, e5821.
- 39 Khodarev NN, Roizman B & Weichselbaum RR (2012) Molecular pathways: interferon/Stat1 pathway: role in the tumor resistance to genotoxic stress and aggressive growth. *Clin Cancer Res* **18**, 3015–3021.
 - 40 Cheon H & Stark GR (2009) Unphosphorylated STAT1 prolongs the expression of interferon-induced immune regulatory genes. *Proc Natl Acad Sci USA* **106**, 9373–9378.
 - 41 Khodarev NN, Beckett M, Labay E, Darga T, Roizman B & Weichselbaum RR (2004) STAT1 is overexpressed in tumors selected for radioresistance and confers protection from radiation in transduced sensitive cells. *Proc Natl Acad Sci USA* **101**, 1714–1719.
 - 42 Chen JJ, Knudsen S, Mazin W, Dahlgaard J & Zhang B (2012) A 71-gene signature of TRAIL sensitivity in cancer cells. *Mol Cancer Ther* **11**, 34–44.
 - 43 Cheriya V, Glaser KB, Waring JF, Baz R, Hussein MA & Borden EC (2007) G1P3, an IFN-induced survival factor, antagonizes TRAIL-induced apoptosis in human myeloma cells. *J Clin Invest* **117**, 3107–3117.
 - 44 Khoo TL, Vangsted AJ, Joshua D & Gibson J (2011) Interferon-alpha in the treatment of multiple myeloma. *Curr Drug Targets* **12**, 437–446.
 - 45 Munshi NC, Hideshima T, Carrasco D, Shamma M, Auclair D, Davies F, Mitsiades N, Mitsiades C, Kim RS, Li C *et al.* (2004) Identification of genes modulated in multiple myeloma using genetically identical twin samples. *Blood* **103**, 1799–1806.
 - 46 Zhan F, Huang Y, Colla S, Stewart JP, Hanamura I, Gupta S, Epstein J, Yaccoby S, Sawyer J, Burington B *et al.* (2006) The molecular classification of multiple myeloma. *Blood* **108**, 2020–2028.
 - 47 Zavidij O, Haradhvala NJ, Mouhieddine TH, Sklavenitis-Pistofidis R, Cai S, Reidy M, Rahmat M, Flaifel A, Ferland B, Su NK *et al.* (2020) Single-cell RNA sequencing reveals compromised immune microenvironment in precursor stages of multiple myeloma. *Nature Cancer* **1**, 493–506.
 - 48 Yoshida A, Funato Y & Miki H (2018) Phosphatase of regenerating liver maintains cellular magnesium homeostasis. *Biochem J* **475**, 1129–1139.
 - 49 Palm W & Thompson CB (2017) Nutrient acquisition strategies of mammalian cells. *Nature* **546**, 234–242.
 - 50 Rathmell JC, Farkash EA, Gao W & Thompson CB (2001) IL-7 enhances the survival and maintains the size of naive T cells. *J Immunol* **167**, 6869–6876.
 - 51 Campeau E, Ruhl VE, Rodier F, Smith CL, Rahmberg BL, Fuss JO, Campisi J, Yaswen P, Cooper PK, Kaufman PD (2009) A versatile viral system for expression and depletion of proteins in mammalian cells. *PLoS ONE* **4**, e6529. <https://doi.org/10.1371/journal.pone.0006529>.
 - 52 Gentleman RC, Carey VJ, Bates DM, Bolstad B, Dettling M, Dudoit S, Ellis B, Gautier L, Ge Y, Gentry J *et al.* (2004) Bioconductor: open software development for computational biology and bioinformatics. *Genome Biol* **5**, R80.
 - 53 Patro R, Duggal G, Love MI, Irizarry RA & Kingsford C (2017) Salmon provides fast and bias-aware quantification of transcript expression. *Nat Methods* **14**, 417–419.
 - 54 Love MI, Huber W & Anders S (2014) Moderated estimation of fold change and dispersion for RNA-seq data with DESeq2. *Genome Biol* **15**, 550.
 - 55 Varet H, Brillet-Gueguen L, Coppee JY & Dillies MA (2016) SARTools: a DESeq2- and EdgeR-based R pipeline for comprehensive differential analysis of RNA-Seq data. *PLoS One* **11**, e0157022.
 - 56 Schindelin J, Arganda-Carreras I, Frise E, Kaynig V, Longair M, Pietzsch T, Preibisch S, Rueden C, Saalfeld S, Schmid B *et al.* (2012) Fiji: an open-source platform for biological-image analysis. *Nat Methods* **9**, 676–682.
 - 57 Chen EY, Tan CM, Kou Y, Duan Q, Wang Z, Meirelles GV, Clark NR & Ma'ayan A (2013) Enrichr: interactive and collaborative HTML5 gene list enrichment analysis tool. *BMC Bioinformatics* **14**, 128.
 - 58 Kuleshov MV, Jones MR, Rouillard AD, Fernandez NF, Duan Q, Wang Z, Koplev S, Jenkins SL, Jagodnik KM, Lachmann A *et al.* (2016) Enrichr: a comprehensive gene set enrichment analysis web server 2016 update. *Nucleic Acids Res* **44**, W90–W97.
 - 59 Rusinova I, Forster S, Yu S, Kannan A, Masse M, Cumming H, Chapman R & Hertzog PJ (2013) Interferome v2.0: an updated database of annotated interferon-regulated genes. *Nucleic Acids Res* **41**, D1040–D1046.